Journal of Applied Fluid Mechanics, Vol. 10, No. 1, pp. 183-197, 2017.
Available online at www.jafmonline.net, ISSN 1735-3572, EISSN 1735-3645.
DOI: 10.18869/acadpub.jafm.73.238.26148

Cross Flow past Circular Cylinder with Waviness in Confining Walls near the Cylinder

R. Deepakkumar[1], S. Jayavel[1†] and S. Tiwari[2]

[1] *Indian Institute of Information Technology Design and Manufacturing Kancheepuram Chennai 600127, India*
[2] *Indian Institute of Technology Madras, Chennai 600036, India*

†*Corresponding Author Email: sjv@iiitdm.ac.in*

(Received January 25, 2015; accepted July 26, 2016)

ABSTRACT

Two dimensional flow past circular cylinder confined by walls with local waviness near the cylinder has been studied. The aim of the present study is to identify the ability of the waviness to control vortex shedding, for which two different waviness configurations such as in-phase configurations (IPC) and out-phase configurations (OPC) are considered. Further, the effect of location of the local waviness with respect to the cylinder has also been studied. Air is the working fluid and the flow is assumed to be laminar and incompressible at Re=200. The finite volume based CFD solver Ansys Fluent (Version 15.0) is used for the computations. Flow characteristics such as drag, lift and Strouhal number are computed. Interesting shedding characteristics and drag reduction are observed due to the presence of local waviness. However, the significant factor is the location of waviness in the confining walls that leads to complete suppression of shedding. Among various locations and configurations of waviness studied, waviness in downstream with OPC3 suppresses the vortex shedding completely with reduced drag.

Keywords: Flow past cylinder; Laminar flow; Wavy-wall confinement; Vortex shedding control.

NOMENCLATURE

A	waviness amplitude of the confining wall
AP	projected area of the cylinder
C_D	drag co-efficient
C_L	lift co-efficient
D	diameter of the cylinder
FSP	front stagnation point
H	distance between the confining walls (along y- direction)
IPC	in-phase configuration
L	length
n	number of grids
OPC	out-phase configuration
P	pressure
Pw	plain-wall
R	radius of the cylinder
Re	Reynolds number
t	time
U	x-component velocity at the inlet
u, v	x- and y-component velocities, respectively
WSS	wall shear stress
x, y	coordinate axes

Greek symbols

β	blockage ratio
λ	waviness length
μ	dynamic viscosity
ρ	density

Subscripts

d	downstream of the domain
max	maximum
r	recirculation
u	upstream of the domain

1. INTRODUCTION

Vortex shedding due to cross flow past a circular cylinder is a common phenomenon in many engineering applications. Many civil structures are subjected to resonance due to alternate shedding which may lead to damage of the entire system, collapse of Tacoma narrows bridge (1940), Millennium bridge (2000) are the well-known examples. The study of vortex shedding and its

control is an active research area. Vortex shedding can be effectively controlled either by blocking the formation of vortex or by minimizing the shedding frequency of already formed unsteady vortices. The active control technique is one of the methods used to control flow and subsequent shedding, Ffowcs Williams and Zhao (1989) used a closed loop acoustic control system and controlled shedding frequency, Chen *et al.* (2013) used suction flow control method, Chen *et al.* (2014) used travelling wave wall, Homescu *et al.* (2002) varied the angular velocity of the rotating cylinder to suppress and control the vortex shedding. Although the active control technique is effective in controlling the vortex shedding, the technique requires continuous supply of external energy in the form of periodic force or injection of additional fluid. On the other hand, passive technique of vortex shedding control requires no external power. For example, cylinder confined by rigid walls effectively controls the shedding characteristics, Shair *et al.* (1963), Chen *et al.* (1995), Sahin *et al.* (2004), Tiwari *et al.* (2006), Semin *et al.* (2009) and Singha *et al.* (2010) have studied the effect of wall confinement on vortex shedding and reported increased drag on the cylinder. Strykowski and Sreenivasan (1990), Mittal and Raghuvanshi (2001) and Dipankar *et al.* (2006) have introduced a secondary small control cylinder in the wake of the main cylinder and effectively controlled the shedding. The presence of splitter plate in the wake also effectively controls the shedding, Kwon and Choi (1996) and Dehkordi and Jafari (2010) have identified the location and length of the splitter plate to reduce drag and lift acting on the cylinder.

The physical structure of the flow does not change with small blockage ratio (β = D/H), Chen *et al*. (1995). Further, Sahin *et al.* (2004) have studied the effect of β on flow past circular cylinder and observed that for the values of β < 0.5, the vortex shedding characteristics were alike to that of unbounded domain (β = 0). From the work of Wu *et al.* (2004), it was observed that the higher blockage ratio results in earlier separation and decrease in separation angle (measured from front stagnation point) due to the local acceleration of flow around the cylinder. However, Karman vortex street was found to be narrow due to the confinement and further increase in β (β > 0.5) leads to re-stabilized steady flow. The work from Anagnostopoulos and Iliadis (1996) and Stansby and Slaouti (1993), reported increased drag and Strouhal number due to confinement. Some of these effects are also observed from the work of Nicolas *et al.* (2011). Thus, wall confinement leads to a stronger stream-wise alignment of vortices and results in coherent and sustained vortices in the downstream. Further, the interaction of vortices formed behind the cylinder and those originated near the confining walls leads to inversion of Von Karman vortices, Camarri and Giannetti (2010) and Singha and Sinhamahapatra (2010). Price *et al.* (2002) have experimentally studied the flow visualization around a circular cylinder near the confining rigid plain wall by varying the gap between the cylinder and the plain wall. They have categorized the gap into four different ranges based on the formation of vortex shedding from both the cylinder and the plain wall. Experimental and numerical works, respectively due to Wang and Tan (2008) and Lei *et al.* (2000) also investigated the wall effect on shedding characteristics. Tabatabaeian *et al*. (2015) used plasma actuator electrodes for controlling the flow structure around a circular cylinder. Son and Cetiner (2016) have studied the drag prediction using mean velocity profiles monitored by digital particle image velocimetry for two-dimensional flows behind circular cylinders in the low Reynolds number regimes (100 < Re < 1250). Also they observed the relation of vortex formation length and wake width to the corresponding drag.

The available literature thus clearly shows the effect of wall confinement on vortex shedding characteristics and especially waviness in the confining walls near the cylinder would be of more interest. The waviness located near the wake region effectively suppresses the shedding has already been reported by present authors (Deepakkumar *et al*. 2015). To the best of authors' knowledge, this is a first attempt on passive control of vortex shedding using local waviness in the confining walls. In the present work, flow past circular cylinder confined with plain walls with local waviness has been computed and the flow characteristics are studied at Reynolds number 200.

2. PROBLEM STATEMENT

The two-dimensional computational study consists of circular cylinder confined between walls with local waviness as shown in Fig.1. In the present work, local waviness is employed as a passive technique to control vortex shedding and the resulting flow characteristics are numerically investigated. The parameters such as length and amplitude (λ = 2D and A = 0.15D) of the waviness are chosen arbitrarily. Based on the results of present work, the effect of λ and A will be studied in the future. To observe the effect of local waviness on vortex shedding, the waviness is placed at different location in the transverse wall boundary as shown in Fig. 2 and the different locations of waviness considered in the present study are discussed in the Section 2.1. The height of the domain is H = 2D. The inlet boundary is place at 6D away from the cylinder to minimize numerical error due to boundary condition and to ensure fully developed flow near the cylinder. On the other hand, to minimize upstream effect of the exit boundary condition, the outlet boundary is placed at 24D away from the cylinder center. Flow past circular cylinder at Re=200 with no-slip plain wall confinement (β=0.5) ensures shedding (Sahin *et al.* 2004). Therefore, in the present work Re=200 has been considered to study the effect of waviness on shedding characteristics. Here Reynolds number is defined as $\mathrm{Re} = \rho U_{\max} D / \mu$. The inlet and outlet boundary are properly placed, so that the disturbance of inlet and outlet boundaries on the flow characteristics near the cylinder can be minimized. In the present study upstream and

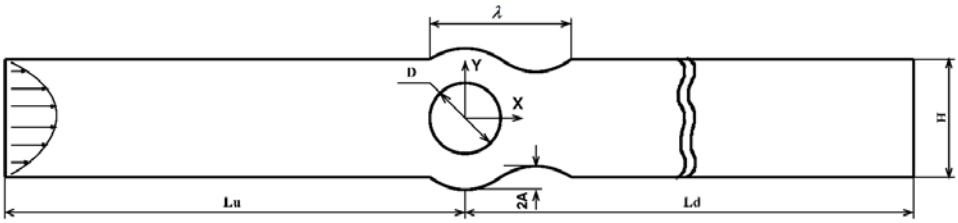

Fig. 1. Computational domain

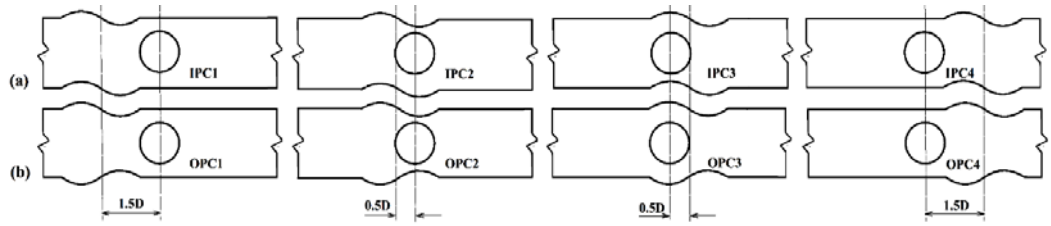

Fig. 2. Various location of waviness near the cylinder (a) IPC (b) OPC.

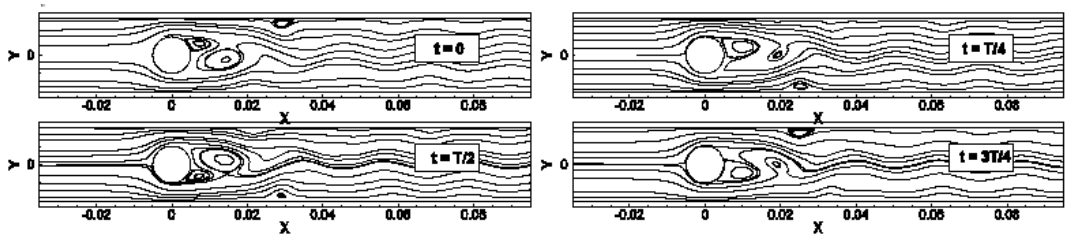

Fig. 3. Streamlines for Plain-wall confinement.

downstream lengths are 6D and 24D, whereas Camarri *et al.* (2010) have taken 12.5D and 35.5D due to low blockage effect, Prasanth *et al.* (2006) used the inlet and outflow boundary at 10D, 25.5 D respectively from the cylinder center. But in present study due high confinement, flow can be stabilized earlier so that the upstream and downstream lengths 6D and 24D are good enough for capturing the vortex shedding characteristics.

2.1 Waviness Configurations

In the present study, the confining walls comprise local waviness near the cylinder as shown in Fig. 1. The length of the waviness (λ) is 2D and it is located at four different positions (viz., IPC1, IPC2, IPC3 and IPC4) as shown in Fig. 2a, where IPC indicates that the waviness in top and bottom wall are in-phase with each other. On the other hand, various locations of waviness with out-phase configuration (OPC) are shown in Fig. 2b. Thus, eight different confining boundaries with waviness are considered in the present study and aimed at identifying a configuration which would lead to suppressed vortex shedding with minimum drag. Flow past circular cylinder with plain-wall (Pw) confinement is taken as the reference case and the corresponding streamline plots at various time instants are presented in Fig. 3. Further computations with waviness (IPC and OPC) are presented and discussed by comparing with the reference case.

2.2 Governing Equations and Boundary Conditions

The flow is assumed to be two-dimensional unsteady with constant fluid properties. As the inlet velocity of the air is very low, the flow is assumed to be incompressible. The mathematical equations governing are given in Eqs. (1) to (3), which include the continuity and momentum equations.

Appropriate boundary conditions are specified at inlet, outlet, top and bottom confining walls and the cylinder surface. The aim of the present work is to exclusively study the effect of local waviness, which requires fully developed flow near the cylinder instead of developing flow. Therefore at the inlet, fully developed parabolic inlet velocity as defined in Eq. (4) has been imposed. The boundary condition at inlet is defined using a user defined function (UDF) embedded in Fluent solver. At the outlet, zero gradients for flow variable as given in Eq. (5) are imposed. The cylinder surface, top and bottom confining walls are enforced with no-slip conditions (Eq. 6).

$$\frac{\partial u}{\partial x}+\frac{\partial u}{\partial y}=0 \tag{1}$$

$$\frac{\partial u}{\partial t}+u\frac{\partial u}{\partial x}+v\frac{\partial u}{\partial y}=-\frac{1}{\rho}\frac{\partial p}{\partial x}+\frac{\mu}{\rho}\left(\frac{\partial^2 u}{\partial x^2}+\frac{\partial^2 u}{\partial y^2}\right) \tag{2}$$

$$\frac{\partial v}{\partial t}+u\frac{\partial v}{\partial x}+v\frac{\partial v}{\partial y}=-\frac{1}{\rho}\frac{\partial p}{\partial y}+\frac{\mu}{\rho}\left(\frac{\partial^2 v}{\partial x^2}+\frac{\partial^2 v}{\partial y^2}\right) \quad (3)$$

$$u=U_{\max}\left(1-\frac{y^2}{(H/2)^2}\right), v=0 \quad (4)$$

$$\frac{\partial u}{\partial x}=0, \frac{\partial v}{\partial x}=0 \quad (5)$$

$$u=0, v=0 \quad (6)$$

2.3 Grid Generation and Solution Methodology

Block structured grid method is used for discretizing the computational domain. The O-grid method is adopted for generating grids around the cylinder. The schematic of the grid is shown in Fig. 4. The flow field variables are computed using the well-established CFD solver Ansys Fluent (15.0). The study is conducted in unsteady region with a time increment of 0.002 based on Courant–Friedrichs–Lewy (CFL) condition and the computations are carried out for 5000 time-steps. The numerical scheme, COUPLED algorithm is employed, which leads to a single matrix equation system for velocity and pressure; thus, requiring a global convergence criterion per time step. The convergence criterion for the residuals are taken as 1×10^{-6}. Second order implicit method is chosen for transient formulation.

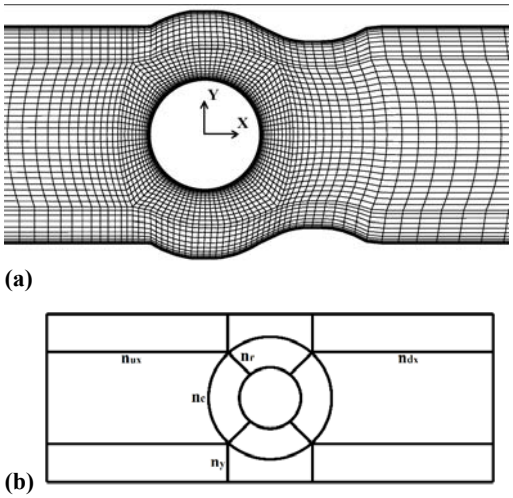

(a)

(b)

Fig. 4. (a) Pictorial view of structured mesh around cylinder and (b) its details.

3. RESULTS AND DISCUSSION

This section includes validation of the present numerical methodology and detailed grid independence study (Section 3.1), the discussion on the effect of location of waviness in IPC and OPC configurations on flow characteristics (Section 3.2 to 3.3), the significance of wavy wall confined cylinder as compared with trough and crest only confined cylinder (Section 3.4) and discussion of phase plot for various configurations (Section 3.5). The study has also been extended to identify the optimized placement of waviness in the confining walls that would lead to suppression of vortex shedding and reduction of drag. The results are presented in the form of coefficients of drag and lift, fluctuation of y-velocity in the wake region, fluctuation of wall shear stress at front stagnation point and streamline plots.

3.1 Validation and Grid Independence Results

Flow past circular cylinder with high confinement (β = 1/2) was studied by Sahin *et al.* (2004), their results are used to validate the numerical methodology of the present work. Fig. 5 shows the effect of Reynolds number on drag coefficient. The results from the present study are compared with those available in the literature and the maximum deviation between the results is 1.82% at Re = 10.

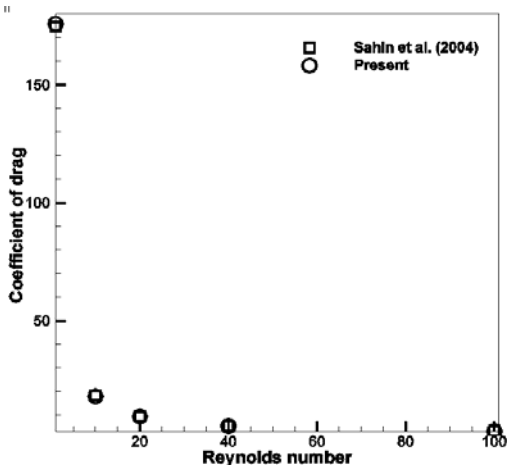

Fig. 5. Comparison of drag coefficient with Reynolds number.

Table 1 Number of nodes in various blocks of different grids

Grid	n_r	n_c	n_y	n_{ux}	n_{dx}	Total nodes	Total cells
G_1	26	33	16	45	302	26053	25550
G_2	40	50	25	68	454	43364	42782
G_3	60	75	38	102	681	139679	138528

The computational domain comprises local waviness in the confining walls which may lead to steep gradients in the flow variables in addition to those normally occur around the cylinder surface. To capture such minute flow characteristics with higher accuracy, refined and optimum grid size is required. Therefore, a thorough grid independence study has been carried out with various grid sizes as listed in Table 1 and the study has been extended for various Reynolds numbers. The effect of grid size on drag coefficient (C_D) and base pressure coefficient (C_{pb}) are shown in Figs. 6a and 6b, respectively. The percentage variation in the values due to change in grid size are shown in Figs. 7a and 7b. The percentage variation in C_D between G_1&G_2 and G_2&G_3 are 0.25 and 0.17, respectively at Re=20, whereas at Re = 200 the variations are 0.17, 0.07. This decrease in variation with increasing Re

is due to change in wake size and C_D is significantly influenced by the wake size. As the wake size increases with increasing Re, the wake region includes more number of nodes. Therefore, drag value when averaged from more number of nodes at higher Re is less dependent on overall grid size. On the other hand, the percentage variation of C_{pb} between G_1&G_2 and G_2&G_3 are 6 and 1.76, respectively at Re = 20 and the percentage variation is found to increase with increasing Reynolds number. It is observed that the nodal value, C_{pb} is more dependent on grid size compared to C_D, a value which is averaged from various nodal points. Thus, the observation of nodal value (C_{pb}) variation with respect to grid size is better choice to conduct grid independence tests and in the present study, the maximum percentage variation of C_{pb} between G_2&G_3 is 3.96. Therefore, based on reduced computational effort and improved solution accuracy G_2 has been chosen as the optimum grid size for further computations.

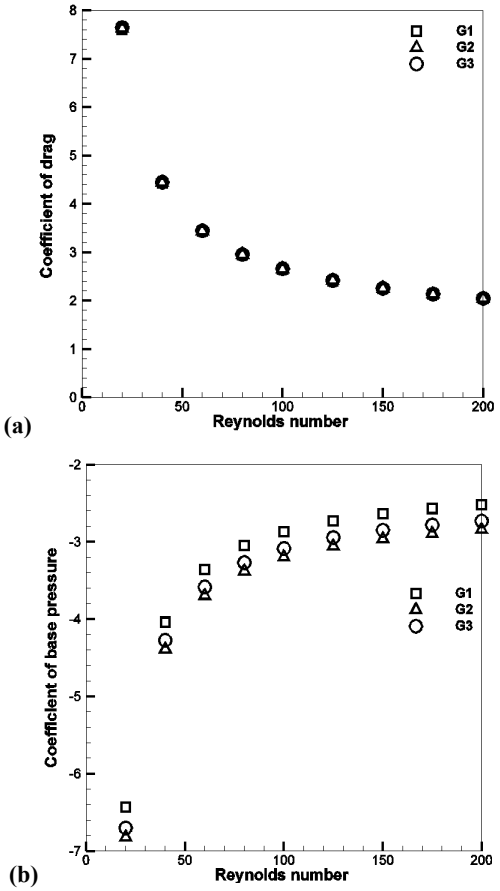

Fig. 6. Effect of grid size on: (a) C_D (b) C_{pb}.

3.2 Flow characteristics Due to Waviness in IPC

Figures 8a and 8b are plotted to observe the variation of C_D and C_L with flow time for various locations of waviness for a time period of 0.5 second and compared with the similar results corresponding to Pw confinement (reference case). The drag force on the cylinder is higher with waviness in IPC, except IPC1. The reduced flow passage due to the presence of wavy-crest leads to flow blockage and pressure build up thereby increased drag. The sudden increase in local confinement also leads to flow acceleration, but this is not accounted from the entire cylinder surface. So the increased total drag is due to the increase of form drag. But in case of IPC1, the approaching flow towards the cylinder is slightly inclined with respect to the main flow direction, thus reduces the wake size. Further, with waviness in IPC1 the presence of two distinguished peaks in the fluctuating C_D is quite interesting and the corresponding FFT of drag-signal is shown in Fig. 9. Although the confining walls are at equidistant from the cylinder center, this contrast nature of two distinguished peaks is also due to the inclined direction of the approaching flow that leads to higher time-averaged flow rate in the gap between bottom wall and cylinder as compared to cylinder and top wall. The instantaneous flow variation with time is shown in Fig. 10a. In the case of Pw confined cylinder, the time-averaged flow rate for one complete cycle is equal along both sides of the cylinder as observed from Fig. 10b. With IPC1, the time-averaged flow past the cylinder is one-sided *i.e.*, increased flow rate in the gap between bottom wall and cylinder creates more pressure and leads to the shift of fluctuating lift-signal towards positive *y*-direction as shown in Fig. 8b as compared to alternating lift of Pw configuration.

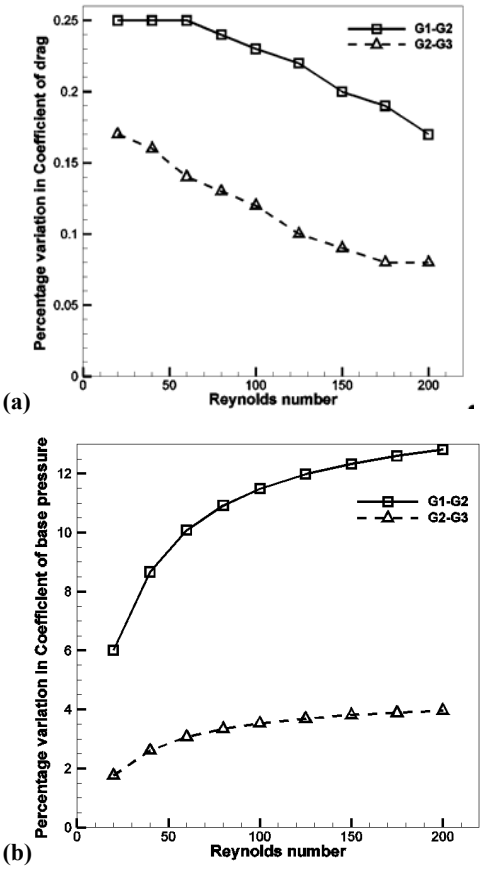

Fig. 7. Percentage variation in the values of flow parameters due to change in grid size (a) C_D (b) C_{pb}.

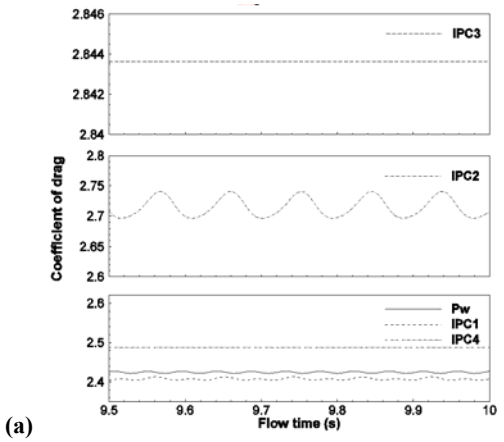

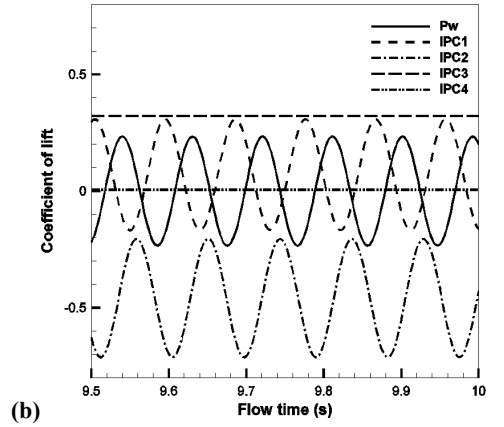

Fig. 8. Effect of location of IPC (a) C_D and (b) C_L.

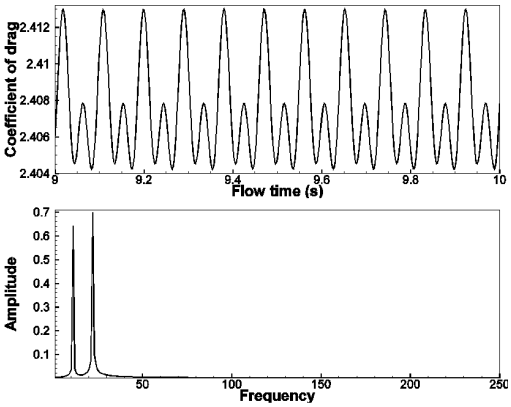

Fig. 9. Fourier spectra of drag coefficient for IPC1.

Vortex shedding characteristics from the cylinder with IPC1 confinement are observed from the streamline plots at various time instants and the corresponding fluctuations in drag and lift coefficients are shown in Fig. 11. The peaks in the drag are observed at the instants t = 9.924s and t = 9.968s (points *S* and *W* in Fig. 11b) when both the vortices are attached with the cylinder surface as shown in Fig. 11a. The two peaks (*S* and *W*) are of unequal magnitude due to reoriented flow direction over the cylinder. The peaks in the drag are due to the attached low pressure vortices (Williamson, 1996). The minimum drag is observed at the instant when any one of the vortices detaches and moves away from the cylinder. At this instant, t = 9.898 s (point Q in Fig. 11b) the reverse flow in the detached region induces a back pressure on the cylinder rear surface, thus the form-drag reduces significantly. Thus, it is clear that the fluctuating drag-signal depends upon the instantaneous position of the vortex in the cylinder wake and the local waviness has an effective control over the phenomena. At the front stagnation point, *y*-component of wall shear provides the detail of flow bifurcation nature, its shift towards either positive or negative side would clearly indicate reorientation of the approaching flow direction. On the other hand *y*-component of wall shear fluctuating in both positive and negative direction indicates the bifurcation of flow on both sides with respect to FSP of the cylinder. If total shear is considered, it may not exactly capture the flow bifurcation nature. Therefore, fluctuating *y*-component of shear stress computed using the velocity gradient, $\partial v/\partial x$ at forward stagnation point is presented in Fig. 13. The shear stress signal monitored at the front stagnation point indicates a shift towards positive *y*-direction for IPC1 due to the inclined approaching flow direction.

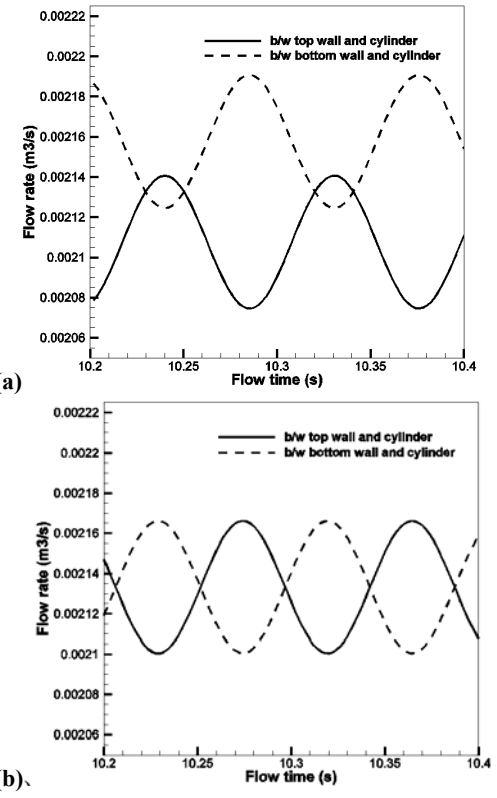

Fig. 10. Time dependent volume flow rate between cylinder and the wall (a) IPC1 (b) Pw.

The suppression of shedding *i.e.*, non-fluctuating lift is observed for the configurations IPC3 and IPC4 (Fig. 8b) but offers more drag on the cylinder as compared to Pw configuration. In the presence of wavy confinement, the percentage increase in drag force is 17.28 and 2.64 for IPC3 and IPC4,

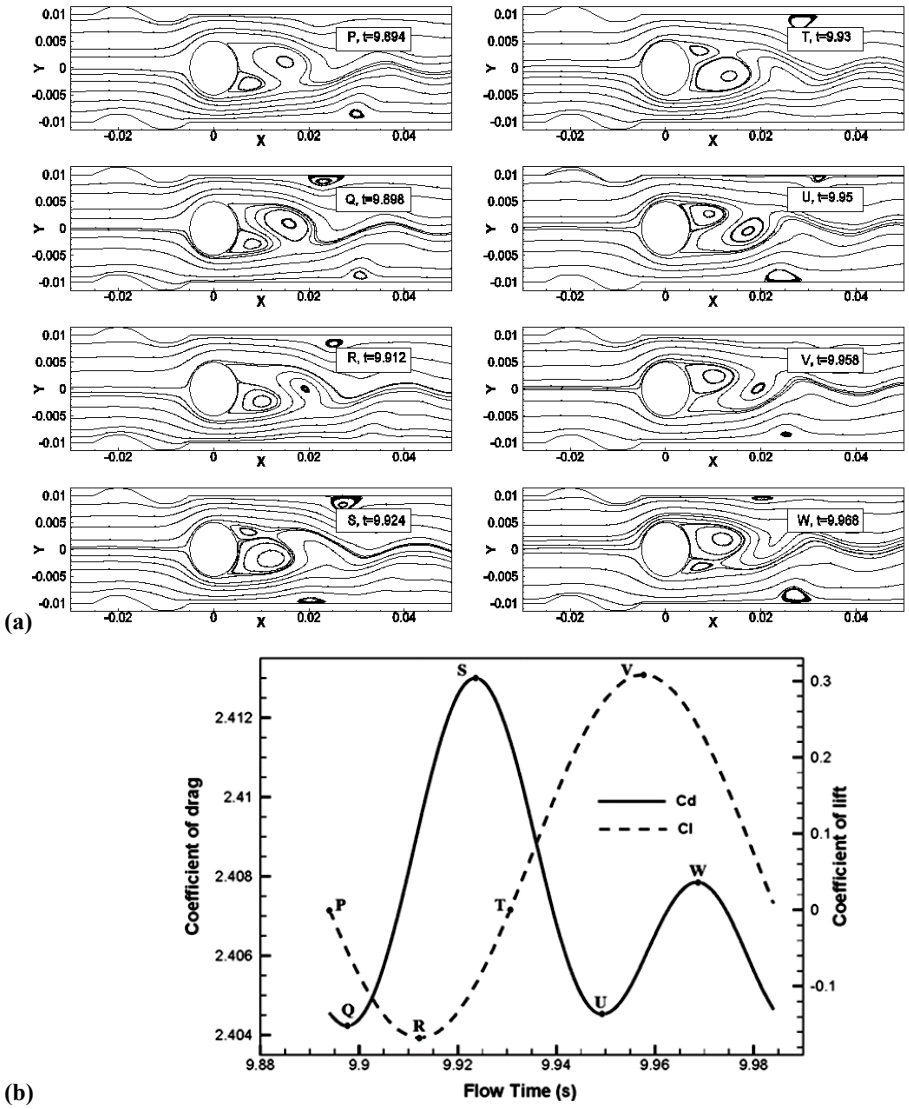

(a)

(b)

Fig. 11. Flow field in presence of waviness in IPC1 (a) Streamline plots at various time instants (b) Variation of drag and lift coefficient with time.

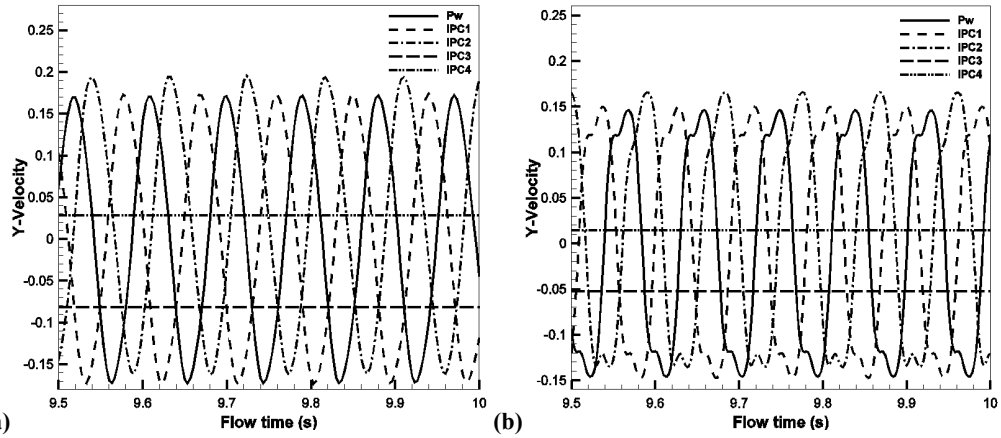

(a) (b)

Fig. 12. Variation of *y*-velocity at various downstream locations (x, 0) (a) x = 2D (b) x = 3D.

respectively. It is also identified that with IPC1 and IPC2, fluctuating lift-signal is shifted either towards positive or negative *y*-direction depending on the approaching flow direction. With IPC1, drag is slightly reduced (0.7%) due to inclined approaching flow. But, with IPC2 drag increases (12.21%) due to increase in local confinement of cylinder. The percentage increase in maximum lift is 32.18 and

Table 2 Effect of placement of waviness due to IPC on C_D, C_L and St

Config.	Mean C_D	Peak to Peak C_L	RMS C_L	Mean C_L	St
Pw	2.424	-0.233 to 0.233	0.165	0	0.355
IPC1	2.407	-0.167 to 0.308	0.181	0.032	0.347
IPC2	2.72	-0.205 to -0.712	0.493	-0.458	0.339
IPC3	2.843	No fluctuation	NA	0.322	No shedding
IPC4	2.488	No fluctuation	NA	0.005	No shedding

Table 3 Effect of placement of waviness due to OPC on C_D, C_L and St

Config.	Mean C_D	Peak to Peak C_L	RMS C_L	Mean C_L	St
Pw	2.424	-0.233 to 0.233	0.165	0	0.355
OPC1	2.382	-0.241 to 0.241	0.171	0	0.355
OPC2	4.302	-0.09 to 0.09	0.064	0	0.347
OPC3	2.050	No fluctuation	NA	0	No shedding
OPC4	2.387	No fluctuation	NA	0	No shedding

205.5%, respectively with IPC1 and IPC2. This drastic rise in lift force with IPC2 is due to unequal confinement of the cylinder and approaching flow direction. It is also noticed that with IPC3, the crest of the waviness suppresses the shedding effectively and results in non-fluctuating lift. The quantitative results such as coefficient of drag, coefficient of lift and Strouhal number are computed at various IPCs and are presented in the Table 2. To study the shedding characteristics, y-component velocities in the wake region are monitored. Figs. 12a and 12b show the fluctuating y-velocity at two different locations (x = 2D and 3D) on the line (x, 0) in the downstream of the cylinder. From this figure it is noticed that there is no fluctuation in y-velocity for IPC3 and IPC4, this ensures the absence of shedding. This effect can also be observed from lift-signals and streamline plots as shown in Figs. 8 and 14, respectively. The nature of y-velocity fluctuation as shown in Fig. 12 with waviness in IPC1 and Pw confinements are similar. However, there is a shift with IPC2 due to local asymmetry in the confinement near the cylinder.

3.3 Flow Characteristics Due to Waviness in OPC

In general, as compared to Pw confinement, unlike IPC, reduced drag is experienced with all OPCs except OPC2 as shown in Fig. 15a. This increased drag in OPC2 is due to the reduced gap between the cylinder and confining walls. This shows the significant role of gap between the cylinder and the confining wall. The drag experienced by the cylinder is very low with OPC3, where the wavy-trough is aligned with the cylinder surface. This reduction in drag is due to two reasons: (i) the decrease in local confinement, which prevents the flow acceleration around the cylinder thereby decreasing the drag. (ii) the flow diversion into the wake takes place in the immediate downstream of the cylinder, which leads to reduction in wake size (Fig. 18).

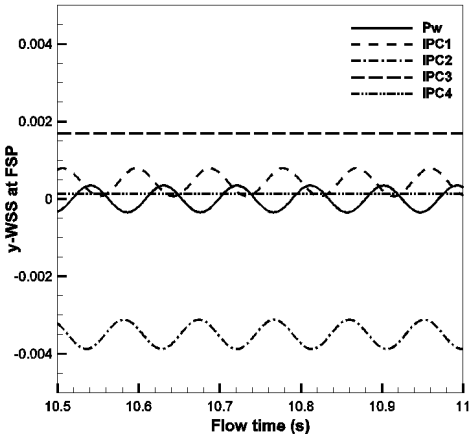

Fig. 13. Variation of *y*-component of wall shear at front stagnation point for various IPCs.

The oscillation of bifurcation point with respect to the forward stagnation point (FSP) is shown in Fig. 16. The point of bifurcation is above the forward stagnation point when the *y*-shear stress is negative and vice-versa. The zero *y*-shear indicates the coincidence of both the bifurcation and the forward stagnation points. As compared to IPC1, there is no secondary peak in drag-signal with OPC1. This is due to the symmetrically bifurcated flow with OPC1. Figure 15b shows the fluctuation of lift coefficients for all OPCs. It is noticed that fluctuation of lift is observed only with OPC1 and OPC2 due to alternate shedding vortices. This is also observed from Fig. 16, where the shear stress symmetrically oscillates with respect to FSP. On the other hand, lift is zero for OPC3 and OPC4, this confirms the absence of shedding, where the *y*-shear stress at FSP with respect to time is also zero (Fig. 16). The quantitative results such as coefficients of drag, lift and Strouhal number are computed with waviness in various OPCs and are presented in the Table 3. As compared to Pw confinement,

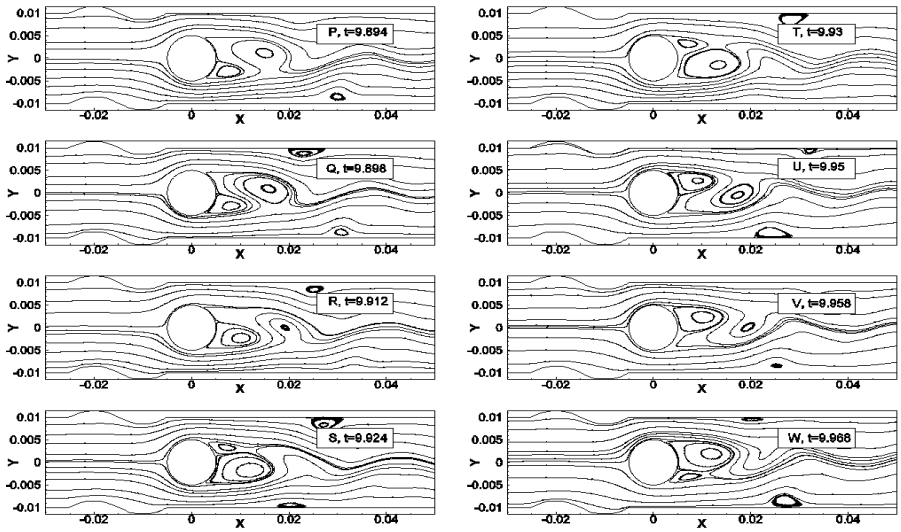

Fig. 14. Streamlines for different location of wavy wall (IPC).

approximately 61.3% of reduction in lift and 77.4% of increase in drag force with OPC2 is observed. On the other hand, OPC1 yields minimum rise (3.43%) in lift force and slight reduction (4.2%) in drag as compared to Pw confinement. Unlike IPC3 & IPC4, zero lift is achieved with decreasing drag force of 15.42% and 1.52% with OPC3 and OPC4, respectively.

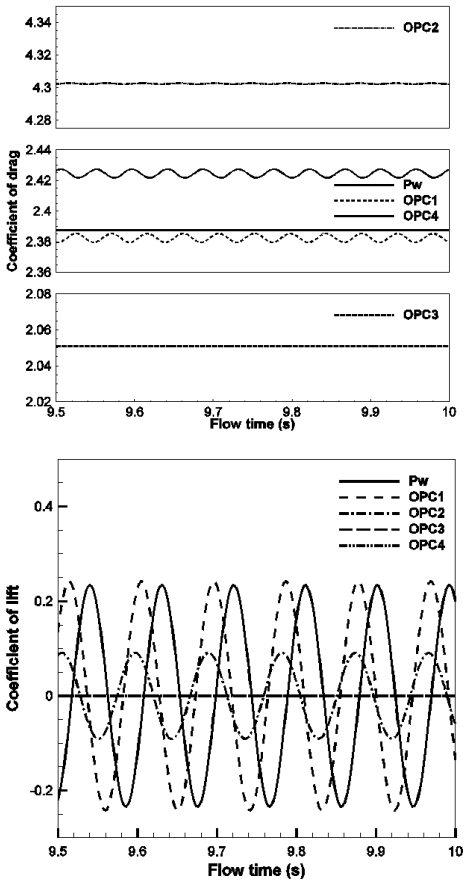

Fig. 15. Effect of location of OPC (a) C_D and (b) C_L.

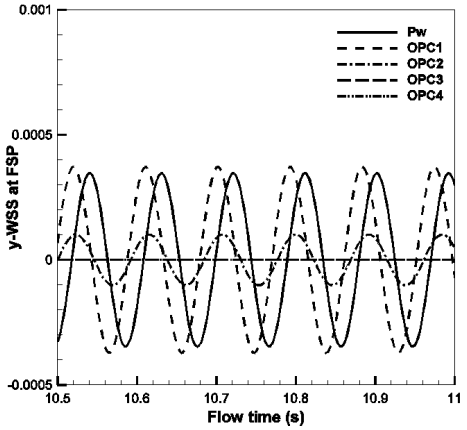

Fig. 16. Variation of *y*-component of wall shear at front stagnation point for various OPCs.

Figures 17a & 17b show the fluctuation of *y*-velocity in the downstream of the cylinder at various locations on the wake centerline. Irrespective of the wavy configuration, (*i.e.*, IPCs or OPCs) waviness in the upstream with respect to the cylinder has less influence on the flow characteristics in the wake. The fluctuation of *y*-velocity with Pw and OPC1 are almost similar. The same effect is also experienced with IPC1 (Fig. 12a and 12b). However, when the waviness position is moved closer to the cylinder (*i.e.*, OPC2), *y*-velocity is significantly influenced. Although waviness is provided near the cylinder (OPC2), shedding occurs. Further movement of the waviness towards the downstream (*i.e.*, OPC3 or OPC4) suppresses the vortex shedding. This observation clearly indicates that the presence of crest in the downstream is essential for the suppression of vortex shedding. The fluctuation of *y*-velocity in OPC2 is comparatively less due to the high local confinement near the cylinder as compared to Pw confined cylinder. The local acceleration of the

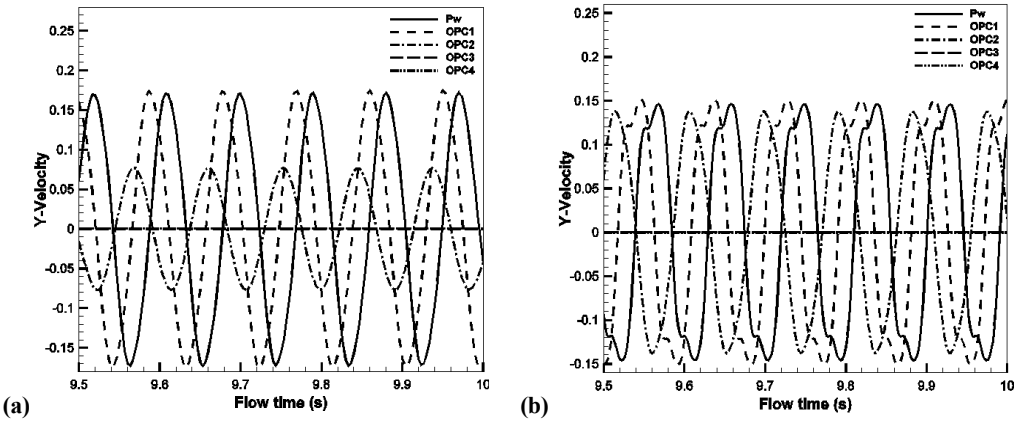

Fig. 17. Variation of *y*-velocity at various downstream location (x, 0) (a) x = 2D (b) x = 3D.

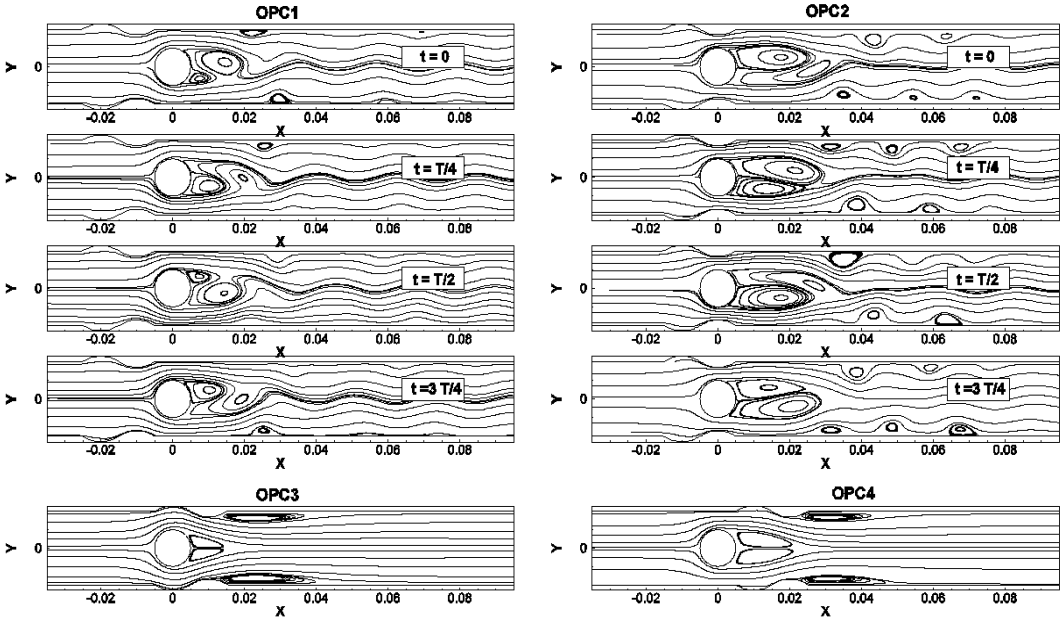

Fig.18. Streamlines for different locations of wavy wall (OPC).

flow through the gap between the cylinder and the confining walls with OPC2 drives the flow parallel to the wake region and reduces flow mixing in the wake and results in low *y*-velocity magnitude in the region as shown in Fig. 17a. This trend is observed closer to the cylinder only (*i.e.,* at $x = 2D$), however, the magnitude of the fluctuating *y*-velocity at $x = 3D$ is similar to Pw confinement. It is noticed that there is no fluctuating *y*-velocity with OPC3 and OPC4, the zero *y*-velocity indicates the steady standing symmetric vortex in the wake region which can also be observed from the streamline plot as shown in Fig. 18. Even though shedding is suppressed with both OPC3 and OPC4 the wake size is drastically reduced with OPC3 compared to OPC4, this reduction is due to the presence of wavy-crest near the wake with OPC3.

3.4 Role of trough and Crest in the local Waviness

In this section, the effect of wall confinement with trough-alone and crest-alone (half-wave) of the optimized configuration OPC3 on shedding characteristics are studied at Re =200 and compared with IPCs and OPCs. The computational domain with trough alone confinement for the study is shown in Fig. 19a and the corresponding flow characteristics such as drag and lift-signals are shown in Figs. 20a and 20b, respectively. The lift-signal ensures the presence of shedding which is further confirmed from the streamline plots as shown in Fig. 21. Although the flow is directed towards the wake due to trough-alone confinement, the dominating inertia force of main flow overcomes the change in flow nature and assists shedding. On the other hand, as discussed in Sections 3.2 and 3.3, OPC3, OPC4, IPC3 and IPC4 show complete suppression in vortex shedding which indicates that suppression of vortex shedding is due to the presence of crest near the wake. It is also noticed that the drag and lift forces with trough-only confined cylinder is significantly reduced due to the reduction in local confinement

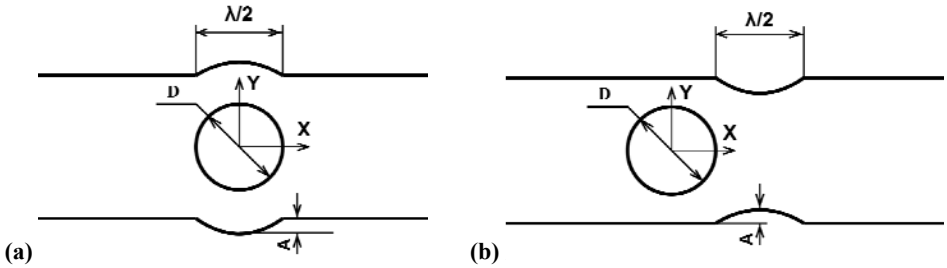

Fig. 19. Computational domain of (a) trough only (b) crest only confined cylinder.

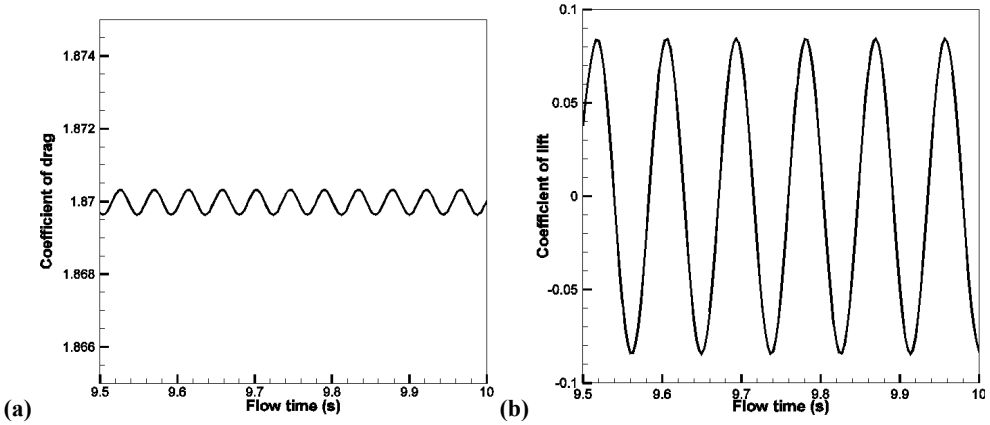

Fig. 20. Effect of trough confined cylinder on C_D and C_L.

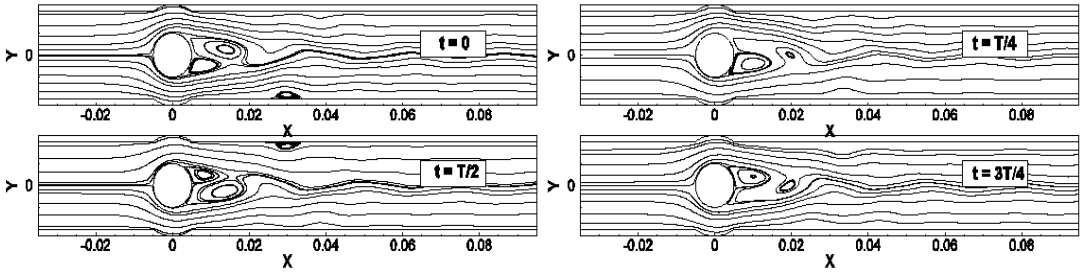

Fig. 21. Streamlines of trough only confined cylinder.

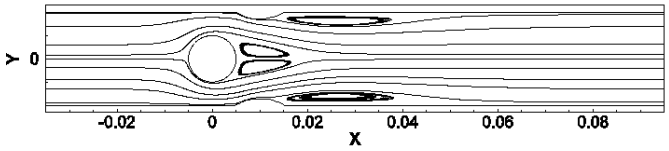

Fig. 22. Streamlines of crest only confined cylinder.

near the cylinder. The mean drag and the maximum lift coefficients are 1.869 and 0.0861, respectively. Thus, trough-only confinement leads to 22.89% and 63.04% decrease in drag and the maximum lift coefficients, respectively compared to Pw confined cylinder. The computational domain with crest alone confinement is shown in Fig. 19b. As discussed earlier, the presence of crest in the downstream of cylinder plays the main role on the complete suppression of shedding. It is observed that there is no shedding from the cylinder surface, therefore there is no fluctuation on drag and lift force as shown in Figs. 23a and 23b respectively. Figure 22 also ensures the steady standing vortices due to the crest alone confined cylinder. On the other hand the drag on the cylinder is increased by 6.6% as compared with plain wall confined cylinder due to higher frictional resistance over cylinder surface in crest only confine cylinder.

As discussed in Section 2.2, the inlet boundary is imposed with fully developed velocity profile (Eq. 4) for all the previous cases. A special case has been considered to study the effect of developing flow, where the flow is allowed to develop in the region of wavy confinement for the optimized location of waviness (OPC3), the resulting flow characteristics are observed. The inlet boundary condition has been modified as uniform velocity and placed at various upstream lengths (L_u = 2D to 6D, with increment of 1D) from the cylinder center. Fig. 24 shows the flow characteristics due to developing flow in the

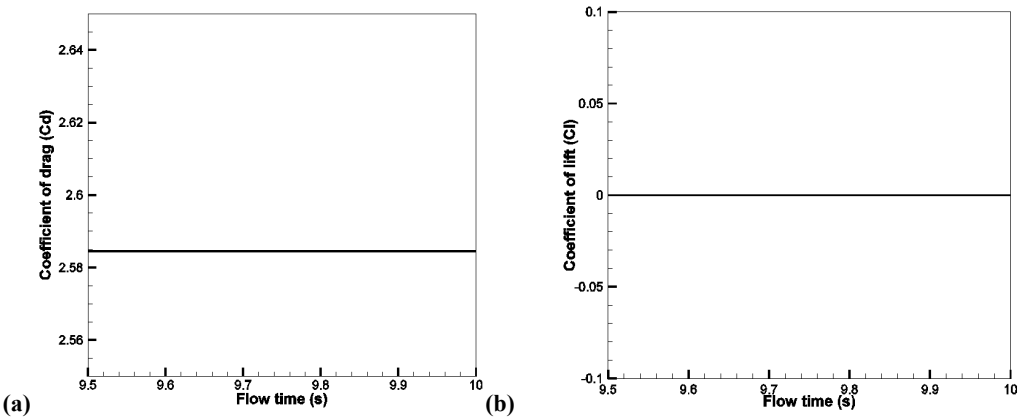

Fig. 23. Effect of crest confined cylinder on (a) C_D and (b) C_L.

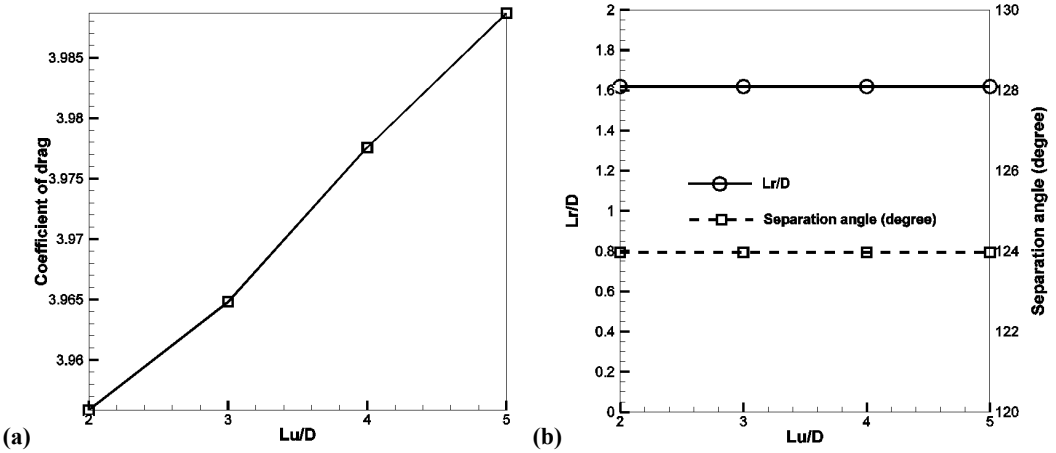

Fig. 24. Effect of developing flow (a) C_D (b) L_r and θ_s.

wavy region for various upstream distances. As the upstream distance increases, the boundary layer thickness increases and leads to increasing local velocity over the cylinder. This increase in local velocity near the cylinder due the developing flow leads to a small increase in drag acting on the cylinder as shown in Fig. 24a. Although the local velocity near the cylinder increases, it has no influence on the recirculation length and angle of separation as observed from Fig. 24b.

3.5 Phase Plot for Different Configurations

Figure 25 shows the phase plot for various wavy configurations that shows the values of C_D and C_L at various instants of time. The occurrence of minimum, average and maximum drag with respect to zero lift can be easily observed from the phase plot. The shift in fluctuating drag is basically due to the effect of confining walls. Considering the case of unconfined flow, minimum drag occurs at zero lift. With increasing confinement at the instant of zero lift, drag gradually increases. With confinement (β = 1/2) (Sahin *et al.* 2004) the average C_D value coincides with zero lift, thereafter with further increase in confinement leads to increasing drag value corresponding to zero lift. Figures 25a to 25f show the phase plot of respectively, Pw, trough-only confined, OPC1, OPC2, IPC1 and IPC2. It is interesting to note that the IPC2 does not have any positive lift as compared to all other configurations. It is identified that phase plot are almost similar in nature except IPC due to asymmetrical wall confinement. Especially for IPC2, there is only one drag cycle with respect to one lift cycle whereas two drag cycle per one lift cycle is observed in all other cases. The fluctuation in lift and drag signals are due to the alternate vortex shedding behind the cylinder. The alternately shedding vortices are of unequal size for IPC1, which leads to asymmetry in the phase plot as shown in Fig. 25c. This unequal size of alternate vortex formation is due to reorientation of the flow direction by the waviness in the confining walls. On the other hand, the single looped phase plot of IPC2 as shown in Fig. 25d is due to unequal local confinement of cylinder, which causes dominating lift along single direction. The resultant force acting on the cylinder due to lift and drag forces is shown in Fig. 26a. It is interesting to note that the resultant force experienced by an unconfined cylinder is less (Deepakkumar and Jayavel, 2014) as compared to flow past cylinder with confinement. Compared to lift, drag is the dominating part contributing to the resultant force. Therefore with confinement, even with decreasing lift the resultant force increases due to considerable

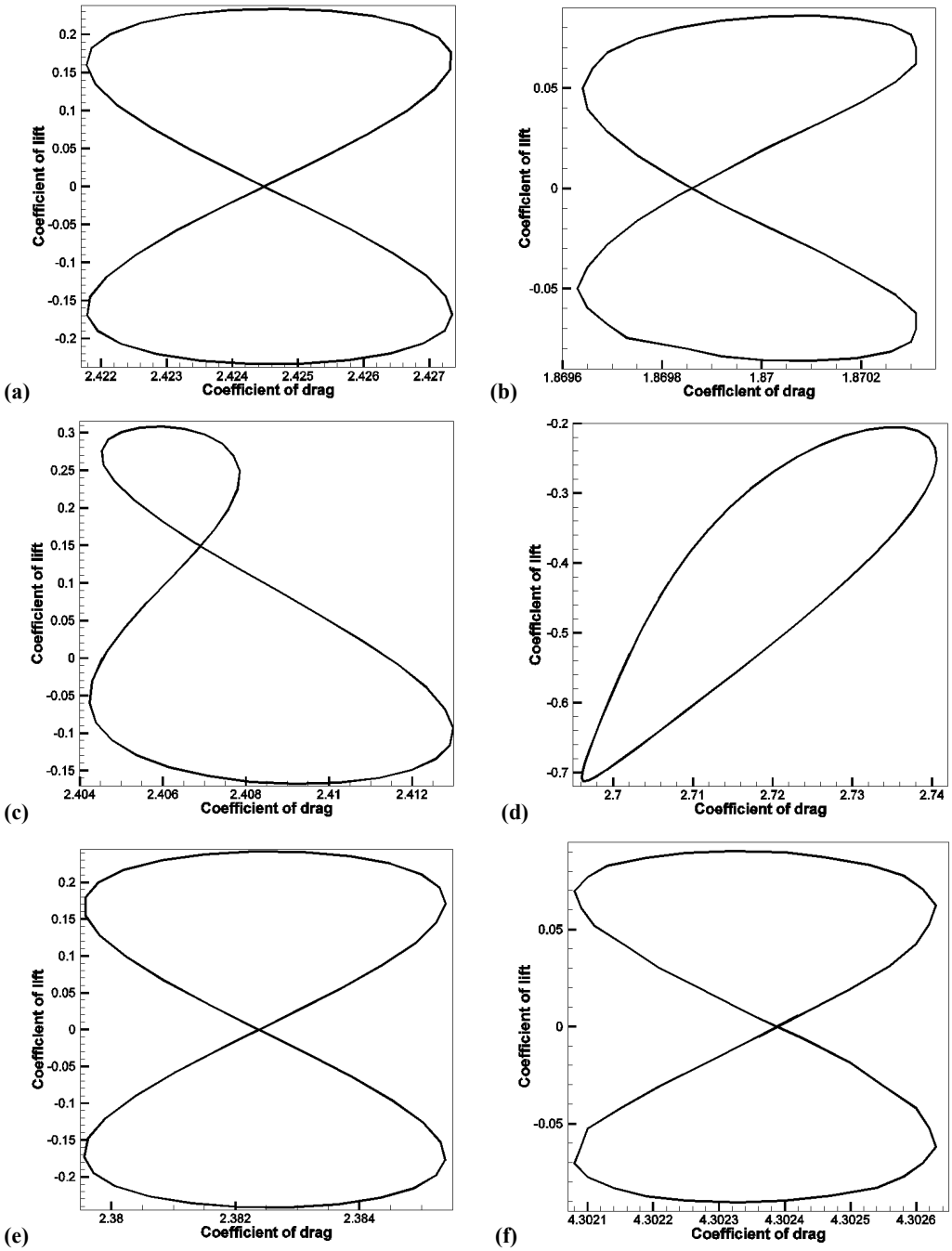

Fig. 25. Phase plot of C_D&C_L for (a) Pw (b) trough only confined (c) IPC1 (d) IPC2 (e) OPC1 and (f) OPC2.

increase in the drag. From Fig. 26b with confinement, the magnitude of fluctuations is observed to be reduced due to controlled shedding and stretched vortices along the flow direction. This reduction is more significant with increasing confinement. This effect can be easily observed from OPC2, where the local confinement is high and subsequently higher resultant force. The gaps between the cylinder and the confining walls significantly influence the direction of the resultant force. This is clearly observed with IPC2 where the trough in the lower confining wall near the cylinder acts as a sudden expansion in the flow passage and creates low pressure, but the crest in the upper confining wall near the cylinder acts as a sudden contraction and induces high pressure on the cylinder. Thus the resultant force acts along negative *y*-direction for the entire shedding period.

4. CONCLUSION

Two dimensional numerical simulations for wall confined flow past circular cylinder are carried out to study the effect of local waviness in confining walls on vortex shedding characteristics at Reynolds number 200. Local waviness in the confining walls has been placed at four different locations with IPC and OPC. In general, for both

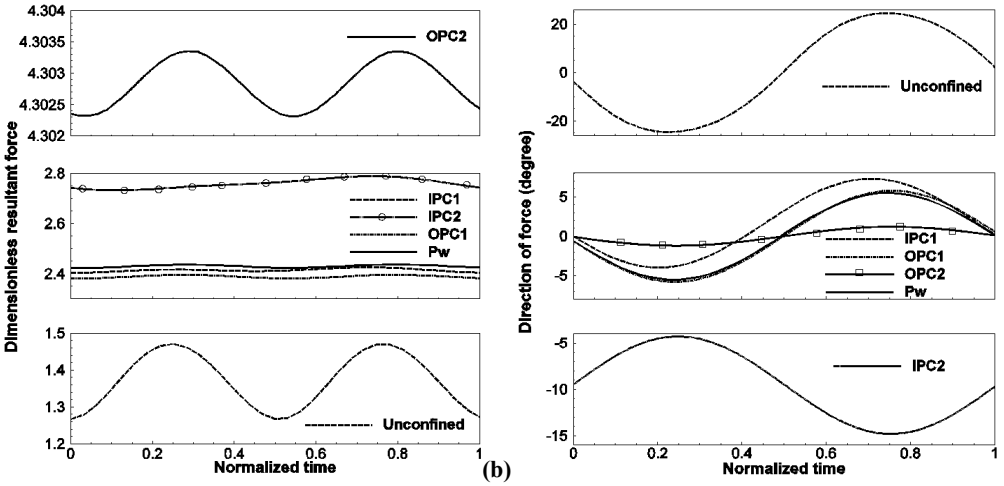

Fig. 26. (a) Resultant force (b) Direction of force for one complete shedding cycle for various configurations.

IPC and OPC, the suppression of shedding is observed with crest of the waviness located near the cylinder wake. The wave center located in upstream (-1.5D) has no influence on vortex shedding, located in front of cylinder (-0.5D) effectively controls the shedding frequency, located in the rear of cylinder (+0.5D) completely suppress the shedding and located in downstream (+1.5D) suppress the shedding with increased drag. The presence of waviness with crest near the cylinder wake reduces flow cross-section, which leads to pressure build up in the wake region. This increase in pressure in the wake region confines the growth of and thereby eliminates shedding of vortex from the cylinder surface. Waviness with OPC in downstream ensures time-averaged lift to be zero. However, flow in presence of local waviness with IPC in downstream leads to positive or negative time-averaged lift depending on the location of the waviness. The locations for both IPC and OPC are identified, which completely suppress the shedding. The optimized location of the waviness and its configuration (OPC3) has been identified based on the reduced drag and complete suppression of vortex shedding. The flow direction approaching the cylinder, the gaps between the cylinder and the confining walls and the location of the crest region are the three major parameters that control the shedding characteristics.

REFERENCES

Anagnostopoulos, P. and G. Iliadis (1996). Numerical study of the blockage effects on viscous flow past a circular cylinder. *International Journal of Numerical Methods in Fluids* 22, 1061-1074.

Camarri, S. and F. Giannetti (2010). Effect of confinement on three-dimensional stability in the wake of a circular cylinder. *Journal of Fluid Mechanics* 642, 477-487.

Chen, J. H., W. G. Pritchard and S. J. Tavener (1995). Bifurcation for flow past a cylinder between parallel planes. *Journal of Fluid Mechanics* 284, 23-41.

Chen, W., H. Hu and H. Li, H. (2013). Suppression of vortex shedding from a circular cylinder by using a suction flow control method. *AIAA Journal,* Vol. 103, 1-10.

Chen, W., Y. Liu, H. Hu, F. Xu and H. Li (2014). Suppression of vortex shedding from a circular cylinder by using a travelling wave wall. *AIAA Journal* 399, 1-11.

Deepakkumar, R. and S. Jayavel (2014, December). Effect of under relaxation factor on convergence rate of computations for flow past circular cylinder. In *Proceedins of International Conference on Theoretical, Applied, Computational and Experimental Mechanics*, IIT Kharagpur, India.

Deepakkumar, R., S. Jayavel and S. Tiwari (2015). "Computational study of fluid flow characteristics past circular cylinder due to confining walls with local waviness. *Proceedings of XXVII IUPAP Conference on Computational Physics: CCP2015*, Paper No. FDCM-O-86, IIT Guwahati, December.

Dehkordi, B. G. and H. H. Jafari (2010). On the Suppression of Vortex Shedding From Circular Cylinders Using Detached Short Splitter-Plates. *Journal of Fluids Engineering* 132, 1-4.

Dipankar, A., T. K. Sengupta and S. B. Talla (2006). Suppression of vortex shedding behind a circular cylinder by another control cylinder at low Reynolds numbers. *Journal of Fluid Mechanics* 573, 171-190.

Ffowcs Williams, J. E. and B. C. Zhao (1989). The active control of vortex shedding. *Journal of Fluids and Structures* 3, 115-122.

Homescu, C., I. M. Navon and Z. Li (2002). Suppression of vortex shedding for flow around a circular cylinder using optimal control. *International Journal of Numerical*

Methods in Fluids 38, 43-69.

Kanaris, N., D. Grigoriadis and S. Kassinos (2011). Three dimensional flow around a circular cylinder confined in a plane channel. *Physics of Fluids* 23(6).

Kwon, K. and H. Choi (1995). Control of laminar vortex shedding behind a circular cylinder using splitter plates. *Physics of Fluids* 8, 479-486.

Lei, C., L. Cheng, S. W. Armfield and K. Kavanagh (2000). Vortex shedding suppression for flow over a circular cylinder near a plane boundary. *Ocean Engineering* 27, 1109-1127.

Mittal, S. and A. Raghuvanshi (2001). Control of vortex shedding behind circular cylinder for flows at low Reynolds numbers. *International Journal of Numerical Methods in Fluids* 35(4), 421-447.

Prasanth, T. K., S. Behara, S. P. Singh, R. Kumar and S. Mittal (2006). Effect of blockage on vortex-induced vibrations at low Reynolds numbers. *Journal of Fluids and Structures* 22, 865-876.

Price, S. J., D. Sumner, J. G. Smith, K. Leong and M. P. Paidoussis (2002). Flow visualization around a circular cylinder near to a plane wall. *Journal of Fluids and Structures* 16(2), 175-191.

Sahin, M., G. Robert and A. Owens (2004). Numerical investigation of wall effects up to high blockage ratios on two-dimensional flow past a confined circular cylinder. *Physics of Fluids* 16(5), 1305-1320.

Semin, B., J. P. Hulin and H. Auradou (2009). Influence of flow confinement on the drag force on a static cylinder. *Physics of Fluids*, 21, pp. 1-9.

Shair, F. H., A. S. Grove, E. E. Petersen and A. Acrivos (1963). The effect of confining walls on the stability of the steady wake behind a circular cylinder. *Journal of Fluid Mechanics* 17, 546-550.

Singha, S. and K. P. Sinhamahapatra (2010). Flow past a circular cylinder between parallel walls at low Reynolds numbers. *Ocean Engineering*, 37, 757-769.

Son, O and O. Cetiner (2016). Drag Prediction in the Near Wake of a Circular Cylinder based on DPIV Data. *Journal of Applied Fluid Mechanics* 9, 1963-1968.

Stansby, P. K. and A. Slaouti (1993). Simulation of vortex shedding including blockage by the random-vortex and other methods. *International Journal of Numerical Methods in Fluids* 17, 1003-1013.

Strykowski, P. J. and R. Sreenivasan (1990). On the formation and suppression of vortex shedding at low Reynolds number. *Journal of Fluid Mechanics* 218, 71-107.

Tabatabaeian, S., M. Mirzaei, A. Sadighzadeh, V. Damideh and A. Shadaram (2015). Experimental Study of the Flow Field around a Circular Cylinder Using Plasma Actuators. *Journal of Applied Fluid Mechanics* 8, 291-299.

Tiwari, S., P. P. Patil, S. Jayavel and G. Biswas (2006, December). Flow field characteristics near first transition for flow past a circular tube confined in a narrow channel. In *Proceedings of the 3rd International and 33rd National Conference on Fluid Mechanics and Fluid Power*, IIT Bombay, India.

Wang, X. K. and S. K. Tan (2008). Near-wake flow characteristics of a circular cylinder close to a wall. *Journal of Fluids and Structures* 24, 605-627.

Williamson, C. H. K. (1996). Vortex dynamics in the cylinder wake. *Annual Review of Fluid Mechanics* 28, 477–539.

Wu, M. H., C. Y. Wen, R. H. Yen, M. C. Weng and A. B. Wang (2004). Experimental and numerical study of the separation angle for flow around a circular cylinder at low Reynolds number. *Journal of Fluid Mechanics* 515, 233-260.